

## THE LUMINOSITY FUNCTIONS AND SIZE DISTRIBUTIONS OF H II REGIONS IN IRREGULAR GALAXIES

ABIGAIL J. YOUNGBLOOD<sup>1</sup> AND DEIDRE A. HUNTER

Lowell Observatory, 1400 West Mars Hill Road, Flagstaff, AZ 86001; ayounbl@brynmawr.edu, dah@lowell.edu

Received 1998 December 1; accepted 1999 February 9

### ABSTRACT

CCD H $\alpha$  images were used to study the properties of H II regions in 29 normal Im galaxies and six blue compact dwarf/starburst irregulars. The H $\alpha$  emission line fluxes were measured and used to construct luminosity functions for each galaxy. For most galaxies, the luminosity function is well represented by a power law. Only two of the 29 Im galaxies have supergiant H II regions, which is probably a result of the small size and small total numbers of H II regions in irregular galaxies. BCDs and starburst galaxies, on the other hand, do not always have supergiant H II regions but may have them even if only a few regions are present. Comparison of the cumulative composite H II luminosity function with that of spiral galaxies shows that the irregulars in our sample do not have an unusually large population of supergiant H II regions relative to the galactic luminosity. Thus, these galaxies will not suffer a disproportionate amount of disruption by the concentration of massive stars within such regions. However, in BCD/starburst galaxies there is an excess of H II regions with luminosities greater than  $10^{38}$  ergs s<sup>-1</sup> compared to Im and Sc galaxies relative to the luminosities of the host galaxies. Most of the H II region luminosity in normal Im galaxies comes from small regions and that in BCD/starburst galaxies from moderately large regions. Over 80% of the H II region luminosity in irregulars is found in complexes of H II regions typically with summed luminosities equivalent to  $\leq 10$  Orion nebulae. Two types of luminosity functions were observed: those that exhibit turnover and those that do not. Those that do exhibit turnover have an average slope of  $-1.5 \pm 0.1$ , and those that do not exhibit turnover tend to be complete to fainter levels, have lower upper luminosity cutoffs, have fewer H II regions, and have shallower slopes of  $-1.0 \pm 0.1$ . If the luminosity function is universal for a galaxy type, this difference suggests the possibility of a break in the luminosity function corresponding to H II regions ionized by single stars and H II regions ionized by clusters of stars. However, we cannot exclude the possibility that the two groups of galaxies are different in terms of their global star formation properties. Diameters of H II regions were also measured and diameter distributions were constructed for each of the galaxies. The diameter distribution was fitted with an exponential and the characteristic diameter  $D_0$  was measured for each galaxy, although this fit did not characterize the distribution very well in most galaxies. The weak correlation between  $D_0$  and the absolute blue magnitude of the galaxy suggested by others is confirmed to be very weak.

*Subject headings:* galaxies: irregular — galaxies: ISM — galaxies: starburst — H II regions

### 1. INTRODUCTION

In order to examine the global and local processes that contribute to star formation in irregular galaxies we have obtained deep H $\alpha$  images of a large sample of irregular galaxies. In the absence of spiral density waves, irregular galaxies enable us to isolate other factors that influence star formation. H $\alpha$  images indicate areas where young, massive stars are located and are used as a tracer of the most recent star formation. The H $\alpha$  images also provide a means to study the properties of individual star-forming regions.

Past research indicates that a galactic H II region luminosity function is best fitted by a power law. Kennicutt, Edgar, & Hodge (1989) compared the luminosity functions of irregular and spiral galaxies and found that the H II region luminosity function shows a strong dependence on Hubble type, which manifests itself in both the shape and slope of the luminosity function. An intriguing suggestion by Kennicutt et al. was that irregulars have more supergiant H II regions ( $L_{\text{H}\alpha} \geq 10^{39}$  ergs s<sup>-1</sup>) than earlier type spirals. We know that stellar initial mass functions (number of stars as a function of the mass of the star) and stellar upper mass limits are the same in smaller, lower metallicity galaxies as

in spirals (Massey, Johnson, & DeGioia-Eastwood 1995a; Massey et al. 1995b; Hunter et al. 1997; Massey 1998; Massey & Hunter 1998), but that does not necessarily imply that the sizes of the star-forming events must be the same in all types of galaxies. In fact, Larson (1983) points out that thicker disks with less shear, such as is the case in irregulars, should allow the growth of larger gas clouds, which in turn could lead to larger star-forming regions. This point is important because, if irregulars do have proportionally larger concentrations of stars of the same age (that is, more supergiant H II regions), one consequence is a greater impact on the interstellar medium by those stars' winds and supernova explosions. This can have profound consequences in rearranging the gas, increasing the inhomogeneity and porosity of the interstellar medium and acting as a feedback to further star formation in these small galaxies.

However, the composite luminosity function constructed by Kennicutt et al. included only six irregular galaxies, at least three of which are or were interacting with other systems (LMC, SMC, NGC 4449). Furthermore, most of the six are relatively high-luminosity systems for irregulars. The motivation for this study, therefore, is to construct a composite H II luminosity function from a larger and more representative sample of irregular galaxies. Here we choose

<sup>1</sup> Current address: Bryn Mawr College, Bryn Mawr, PA 19010-2899.

to exclude all galaxies that show signs of interaction in order to isolate internal star formation processes. The H II region luminosity function will provide insights into how the process of star formation might be different in irregular galaxies, in particular in the formation of giant and super-giant H II regions.

We have also constructed diameter distributions for each of the galaxies in our sample. The diameter distribution has been found to be represented by an exponential function, the slope of which yields the characteristic diameter  $D_0$  of the ensemble of H II regions for the galaxy. This relationship was first proposed by van den Bergh (1981), and since then has been pursued by many additional studies, especially for irregulars (Hodge 1983; Hodge, Lee, & Kennicutt 1989a, 1989b; Hodge & Lee 1990; Strobel, Hodge, & Kennicutt 1991; Hodge, Kennicutt, & Strobel 1994a; Hodge, Strobel, & Kennicutt 1994b; Miller & Hodge 1994). Strobel et al. (1991) have also suggested that there is a weak correspondence between  $D_0$  and the absolute blue magnitude of a galaxy. We have, therefore, used our sample of galaxies to further explore the relationship between the characteristic size scale for the H II region diameter distribution and the absolute magnitude of the galaxy, the universality of the diameter distribution, and the validity of the characteristic diameter as a physically meaningful parameter to describe the properties of H II regions.

In this paper we construct luminosity and diameter functions for the H II regions in 29 nearby Im-type galaxies. We have restricted our sample to those galaxies with H $\alpha$  images whose resolution is high enough and noise low enough to match the work on spirals by Kennicutt et al. (1989) and on irregulars by Hodge and collaborators. We also include three galaxies classed as blue compact dwarfs (BCDs) and three irregulars that are said to be undergoing bursts of star formation. The three BCDs are irregular-like in size and abundances (to be discussed elsewhere) but have high surface brightness and intense emission lines, and they are thus likely to have higher than typical levels of star formation activity (but see Lynds et al. 1998). Therefore, these six galaxies allow us to examine for comparison the H II region characteristics in irregular galaxies with heightened levels of star formation.

We recognize that the diameter and luminosity of an H II region evolve with age of the region, as the star-forming region gnaws its way out of the molecular cloud and then blows the cloud away. For example, the H $\alpha$  luminosity may be low early on as the star-forming region is just emerging from obscuration within the cloud, rise as the H II region reaches its peak optical visibility, and drop after it becomes density-bounded and the most massive stars begin to die off. However, we believe that the diameter and luminosity functions are, nevertheless, useful as snapshots of the ensemble of regions in the galaxy. Probably, though, these distributions have the most meaning when the formation of star-forming regions is in a steady state, which is not the case in a starburst situation. See Oey & Clarke (1998) for a thorough investigation into the effects of an aging population on the H II luminosity function.

## 2. THE DATA

### 2.1. The Observations

The H $\alpha$  images were obtained over 22 observing runs from 1988 to 1998 with the Perkins 1.8 m telescope at

Lowell Observatory and 800  $\times$  800 TI CCDs. Some of these images are described by Hunter, Hawley, & Gallagher (1993). The galaxies were imaged through a narrowband H $\alpha$  filter, usually with a FWHM  $\sim$  30 Å, and a continuum-only off-band filter centered at 6440 Å with a FWHM of 95 Å. Multiple images of up to 3000 s each were obtained and combined to remove cosmic rays. The off-band image was shifted, scaled, and subtracted from the H $\alpha$  image to remove the stellar continuum. The H $\alpha$  emission was calibrated using the known H $\alpha$  flux from H II regions NGC 2363 (Kennicutt, Balick, & Heckman 1980) and NGC 604 (Hunter, unpublished spectrophotometry) and using spectrophotometric standard stars. These objects agreed with each other to 4%. Furthermore, the calibrations remained constant to 8% for a given filter over many observing runs. The H $\alpha$  flux has been corrected for the shift of the bandpass with temperature, contamination by the [N II]  $\lambda$ 6584 emission line in the bandpass ( $\leq$  1% correction), and foreground reddening. Sky was subtracted from the image most often using a two-dimensional fit to the background.

### 2.2. The H II Region Photometry

Table 1 lists the galaxies chosen for this study along with distances that we used and a few global properties. Distances were determined using independent means whenever available, or using a Hubble constant of 65 km s $^{-1}$  Mpc $^{-1}$ , corrected for local motions, when no other distance measurement was available. All of the galaxies selected were nearby ( $D \leq 9$  Mpc) to ensure detection of smaller regions and to minimize crowding.

So that our results would be directly comparable to those determined for spiral galaxies, we have adopted methods similar to those used in previous studies. First, all images were smoothed to a common linear resolution of 30–75 pc, independent of their original distance or resolution. This was done to ensure that the effects due to crowding and blending acted equally in all images and this was the resolution window used by Kennicutt et al. (1989). For many of the images smoothing was unnecessary due to the seeing limit of the image, and images whose resolution was greater than 75 pc were eliminated from the study.

Second, the H II region boundaries were selected by eye from the continuum-subtracted H $\alpha$  image after clipping all images to an H $\alpha$  surface brightness of  $3 \times 10^{-17}$  ergs s $^{-1}$  cm $^{-2}$  arcsec $^{-2}$ . This surface brightness level was chosen to ensure uniformity in boundaries and to match the level used by Strobel et al. (1991) in their study of irregular galaxy diameter functions. Images in which the noise level was significantly higher than this clipping level were excluded from the sample. However, in a few cases we smoothed images where smoothing the image significantly improved the signal-to-noise without pushing the image beyond the resolution window. We included all H II regions that could be distinguished above this background. Suspicious objects were examined in off-band images to ensure that residual stars and other objects were not falsely identified. An unsharp masking technique was used as an aid to better distinguish separate objects in crowded regions, although the technique was used only for identification purposes. The H II region fluxes were measured to this surface brightness level on the clipped images. We were concerned that by clipping the images we may have biased fluxes of some faint regions in the positive direction. However, experi-

TABLE 1  
THE GALAXIES

Galaxy	Other Names <sup>a</sup>	$D$ (Mpc)	$M_B$ <sup>b</sup>	$E(B-V)_f$ <sup>c</sup>	$\log \text{SFR}/\text{Area}^d$
Im-Type Galaxies					
DDO 43 .....	PGC 21073, UGC 3860, A0724+40, KIG 0190	5.5	-14.27	0.055	-2.91
DDO 46 .....	PGC 21585, UGC 3966, A0738+40	5.5	-15.44	0.053	-3.14
DDO 47 .....	PGC 21600, UGC 3974, A0739+16	2.8	-14.15	0.023	-3.24
DDO 50 .....	PGC 23324, UGC 4305, Holmberg II, Arp 268, VIIZw 223, A0813+70, KUG 0814+708, KIG 0239, IRAS F08140+7052	3.2	-16.93	0.023	-2.90
DDO 53 .....	PGC 24050, UGC 4459, A0829+66, VIIZw 238, IRAS F08295+6621, VV 499	1.8	-12.31	0.025	-2.52
DDO 69 .....	PGC 28868, UGC 5364, A0956+30, Leo A, Leo III	1.6	-13.51	0.0	-4.03
DDO 70 .....	PGC 28913, UGC 5373, A0957+05, Sextans B, KIG 0388	1.4	-14.35	0.013	-3.44
DDO 75 .....	PGC 29653, UGCA 205, A1008-04, Sextans A, IRAS F10085-0427	1.4	-14.24	0.018	-2.64
DDO 87 .....	PGC 32405, UGC 5918, VIIZw 347, A1046+65	6.7	-14.44	0.0	-3.50
DDO 101 .....	PGC 37449, UGC 6900, A1153+31	9.0	-15.42	0.008	-3.52
DDO 115 .....	PGC 39142, UGC 7254, IC 3059	3.2	-13.26	0.005	-3.06
DDO 125 .....	PGC 40904, UGC 7577, A1225+43	3.8	-15.47	0.0	-3.54
DDO 126 .....	PGC 40791, UGC 7559, A1224+37	3.8	-14.11	0.0	-3.20
DDO 133 .....	PGC 41636, UGC 7698, A1230+31	5.3	-16.05	0.003	-3.82
DDO 154 .....	PGC 43869, NGC 4789A, UGC 8024	4.0	-14.52	0.008	-3.41
DDO 155 .....	PGC 44491, GR8, UGC 8091, A1256+14, LSBC D646-07, VV 558	1.1	-10.98	0.01	-2.02
DDO 165 .....	PGC 45372, UGC 8201, A1304+67, IIZw 499, Mailyan 82	2.6	-14.73	0.01	-3.75
DDO 167 .....	PGC 45939, UGC 8308, A1311+46	3.7	-12.84	0.0	-3.05
DDO 168 .....	PGC 46039, UGC 8320, A1312+46	3.5	-15.43	0.0	-3.07
DDO 169 .....	PGC 46127, UGC 8331, A1313+47	5.3	-14.44	0.0	-4.07
DDO 183 .....	PGC 49158, UGC 8760, A1348+38	4.1	-14.12	0.0	-3.71
DDO 185 .....	PGC 49448, UGC 8837, Holmberg IV, A1352+54	4.0	-14.61	0.0	-3.44
DDO 187 .....	PGC 50961, UGC 9128, A1413+23	4.7	-14.39	0.0	-3.52
DDO 216 .....	PGC 71538, UGC 12613, A2326+14, Peg DIG, Pegasus Dwarf	2.5	-14.29	0.023	-4.45
WLM .....	PGC 143, UGCA 444, DDO 221, A2359-15, Wolf-Lundmark-Melotte	1.0	-14.46	0.018	-3.79
NGC 1156 .....	PGC 11329, UGC 2455, KIG0121, VV 531, IRAS F02567+2502	7.0	-18.00	0.165	-1.99
NGC 2366 .....	PGC 21102, UGC 3851, DDO 42, IRAS F07234+6917	3.2	-16.69	0.043	-2.71
NGC 3738 .....	PGC 35856, UGC 6565, Arp 234, KUG 1133+548, IRAS F11330+5448	4.6	-16.60	0.0	-2.26
UGC 8508 .....	PGC 47495, IZw 60	2.6	...	0.0	-2.83
BCD and Starburst Galaxies					
IC 10 .....	PGC 1305, UGC 192, IRAS F00177+5900	1.0	-16.31	0.65	-1.48
NGC 1569 .....	PGC 15345, UGC 3056, Arp 210, VIIZw 16, IRAS F04260+6444	2.5	-17.65	0.508	-1.07
NGC 4214 .....	PGC 39225, UGC 7278, KUG 1213+366, IRAS F12131+3636	4.8	-18.58	0.0	-2.42
Haro 29 .....	PGC 40665, UGCA 281, Mrk 209, IZw 36, A1223+48	5.4	-14.28	0.0	-1.57
Mrk 178 .....	PGC 35684, UGC 6541, A1130+49	4.6	-14.23	0.0	-2.21
VIIZw 403 .....	PGC 35286, UGC 6456, VV 574, A1124+79, IRAS F11246+7916	4.5	-14.68	0.023	-2.25

<sup>a</sup> This is not a comprehensive list of identifications; we do not include, for example, CGCG, MCG, NGP9, ZOAG, LGG, AM, UKS, SGC, JB, GSC, or CG entries. Alternative names were found using NED.

<sup>b</sup> From de Vaucouleurs et al. 1991.

<sup>c</sup> Luminosities are corrected for foreground reddening using  $E(B-V)$ -values given by Burstein & Heiles 1984 and the interstellar reddening curve of Cardelli, Clayton, & Mathis 1989.

<sup>d</sup> Star formation rate in units of  $M_\odot \text{ yr}^{-1}$  per  $\text{kpc}^2$ . The area of the galaxy is determined from  $D_{25}$ , the diameter measured to a surface brightness of 25 magnitudes per  $\text{arcsec}^2$ , in de Vaucouleurs et al. 1991. The  $\text{H}\alpha$  luminosity used to construct the SFR is corrected for foreground reddening and internal reddening determined from spectroscopy of individual H II regions (Hunter & Hoffman 1999).

TABLE 2  
H II REGION MEASUREMENTS

Galaxy	$N_{\text{H II}}^a$	$\log L_{\text{limit}}^b$	$D_0^c$ (pc)	$\alpha^d$	$\log L_{\text{upper}}^e$ (ergs s $^{-1}$ )	$D_{\text{upper}}^f$ (pc)	$f(30 \text{ Dor})^g$	$f(\text{Orion})^h$	$f(\text{H}\alpha \text{ Included})^i$	LF $^j$ Type
Im-Type Galaxies										
DDO 43 .....	26	36.6	39 $\pm$ 4	-1.77 $\pm$ 0.16	37.91	234	0.0	0.44	0.56	Turnover
DDO 46 .....	19	36.4	44 $\pm$ 13	-1.39 $\pm$ 0.15	38.01	182	0.0	0.22	0.44	Turnover
DDO 47 .....	67	36.0	27 $\pm$ 2	-1.73 $\pm$ 0.12	37.29	118	0.0	0.66	0.41	Turnover
DDO 50 .....	101	36.6	52 $\pm$ 3	-1.25 $\pm$ 0.07	38.70	283	0.0	0.05	0.63	Turnover
DDO 53 .....	25	36.0	37 $\pm$ 6	-1.49 $\pm$ 0.09	37.85	161	0.0	0.40	0.71	Turnover
DDO 69 .....	15	35.2	54 $\pm$ 5	-0.99 $\pm$ 0.06	36.93	151	0.0	0.95	0.47	No
DDO 70 .....	18	35.4	63 $\pm$ 2	-1.02 $\pm$ 0.11	37.28	143	0.0	0.50	0.53	No
DDO 75 .....	34	36.0	56 $\pm$ 4	-1.10 $\pm$ 0.14	38.01	258	0.0	0.17	0.49	No
DDO 87 .....	16	36.6	109 $\pm$ 6	-1.45 $\pm$ 0.07	38.06	453	0.0	0.21	0.55	Turnover
DDO 101 .....	12	36.8	89 $\pm$ 20	-1.00 $\pm$ 0.00	37.61	316	0.0	0.27	0.23	No
DDO 115 .....	19	36.0	24 $\pm$ 3	-1.40 $\pm$ 0.24	36.83	126	0.0	0.87	0.27	Turnover
DDO 125 .....	9	36.2	132 $\pm$ 8	-0.97 $\pm$ 0.09	37.76	370	0.0	0.04	0.33	No
DDO 126 .....	20	36.2	68 $\pm$ 6	-1.07 $\pm$ 0.09	38.03	443	0.0	0.08	0.63	No
DDO 133 .....	40	36.4	121 $\pm$ 7	-1.21 $\pm$ 0.10	38.11	459	0.0	0.08	0.57	No
DDO 154 .....	74	36.4	90 $\pm$ 4	-1.45 $\pm$ 0.27	37.42	414	0.0	0.34	0.55	Turnover
DDO 155 .....	6	36.4	18 $\pm$ 5	-1.88 $\pm$ 0.00	37.00	87	0.0	0.75	0.55	Turnover
DDO 165 .....	11	35.6	62 $\pm$ 6	-1.22 $\pm$ 0.21	37.25	205	0.0	0.49	0.27	Turnover
DDO 167 .....	7	36.6	56 $\pm$ 2	-0.91 $\pm$ 0.11	37.56	202	0.0	0.18	0.58	No
DDO 168 .....	58	37.0	42 $\pm$ 2	-2.67 $\pm$ 0.17	37.49	239	0.0	0.50	0.48	Turnover
DDO 169 .....	5	36.4	163 $\pm$ 49	-1.00 $\pm$ 0.00	37.78	290	0.0	0.02	1.00	No
DDO 183 .....	25	36.2	40 $\pm$ 5	-1.30 $\pm$ 0.16	37.19	167	0.0	0.41	0.67	Turnover
DDO 185 .....	33	36.8	71 $\pm$ 4	-1.54 $\pm$ 0.12	37.89	318	0.0	0.19	0.65	Turnover
DDO 187 .....	7	36.6	99 $\pm$ 9	-0.83 $\pm$ 0.07	37.24	256	0.0	0.31	0.34	No
DDO 216 .....	6	35.8	87 $\pm$ 8	-0.60 $\pm$ 0.15	36.45	205	0.0	0.88	0.20	No
WLM .....	30	35.4	36 $\pm$ 3	-0.84 $\pm$ 0.12	37.29	165	0.0	0.53	0.57	No
NGC1156 .....	108	37.4	92 $\pm$ 2	-1.50 $\pm$ 0.09	39.71	588	0.33	0.001	0.68	Turnover
NGC2366 .....	105	36.6	55 $\pm$ 1	-1.45 $\pm$ 0.09	39.80	522	0.64	0.02	0.88	Turnover
NGC3738 .....	18	37.8	41 $\pm$ 4	-1.50 $\pm$ 0.30	38.89	248	0.0	0.0	0.70	Turnover
UGC8508 .....	9	37.0	49 $\pm$ 4	-2.40 $\pm$ 0.50	37.55	185	0.0	0.32	0.54	Turnover
BCD and Starburst Galaxies										
IC10 .....	97	36.6	27 $\pm$ 2	-1.43 $\pm$ 0.09	38.68	159	0.0	0.06	0.55	Turnover
NGC1569 .....	31	38.0	34 $\pm$ 3	-1.38 $\pm$ 0.16	39.90	187	0.57	0.00	0.49	Turnover
NGC4214 .....	204	36.8	84 $\pm$ 1	-1.48 $\pm$ 0.04	39.52	528	0.47	0.01	0.56	Turnover
Haro29 .....	9	37.4	110 $\pm$ 8	-1.15 $\pm$ 0.13	39.58	513	0.90	0.01	0.94	Turnover
Mrk178 .....	21	36.8	51 $\pm$ 2	-1.41 $\pm$ 0.15	38.78	464	0.0	0.05	0.75	Turnover
VIIZw 403 .....	15	37.4	55 $\pm$ 7	-1.34 $\pm$ 0.17	38.71	234	0.0	0.01	0.63	Turnover

<sup>a</sup> The total number of H II regions identified on our images.

<sup>b</sup> The H II region detectability limit.

<sup>c</sup> The characteristic H II region diameter, determined from fitting an exponential to the cumulative diameter function.

<sup>d</sup> Power-law index determined in the fit to the H II region luminosity function.

<sup>e</sup> The highest luminosity of an H II region measured in each galaxy.

<sup>f</sup> The largest diameter H II region measured in each galaxy.

<sup>g</sup> Fraction of the total luminosity of all the measured H II regions that is in H II regions with luminosities equal to or greater than  $10^{39}$  ergs s $^{-1}$ .

<sup>h</sup> Fraction of the total luminosity of all the measured H II regions that is roughly comparable in luminosity to Orion and a little less ( $10^{36}$ – $10^{37}$  ergs s $^{-1}$ ).

<sup>i</sup> Fraction of the integrated H $\alpha$  luminosity that is measured in the identified H II regions.

<sup>j</sup> Luminosity function type. A luminosity function exhibiting a turnover in its luminosity function is referred to as of type “Turnover” and those showing no turnover are referred to as of type “No Turnover” in the text.

ments with artificial H II regions suggest that clipping may more often bias the faintest regions toward even fainter values.

Large H II complexes, shells, loops, filaments, and diffuse emission made identification of regions challenging. To provide consistency in all images, a uniform method was adopted for identifying regions with these morphologies. Within H II complexes, embedded regions corresponding to separate peaks of emission were separated. This method was adopted as most physically meaningful because it ensures that individual H II regions most nearly correspond with separate excitation sources. This method is also consistent with the philosophy used by Hodge and collaborators

in identifying H II regions.

Shells and loops were included as H II regions, although they represent more evolved star formation regions. However, knots along the edges of shells were treated as separate regions. Studies of H II regions in the LMC (Oey & Massey 1995), for example, indicate that star formation events on the edges of shells are often triggered by the expansion of the older shell into the surrounding region. In this situation, therefore, they are younger and should be treated as a separate event.

Filaments of ionized gas and general diffuse emission in the galaxies were not included as separate regions because they do not have their own ionizing stars but are usually

ionized by escaping photons from nearby H II regions. The ratio of total luminosity found by summing the identified H II regions to the integrated H $\alpha$  luminosity found from single aperture photometry on the unclipped H $\alpha$  image is listed in Table 2, and these values spanned a wide range. On average, identified H II region luminosities made up about 50% of the total H $\alpha$  luminosity, while the other 50% was composed of diffuse emission and filaments not included in H II regions.

Fluxes of each H II region were integrated to the surface brightness level of  $3 \times 10^{-17}$  ergs s $^{-1}$  cm $^{-2}$  arcsec $^{-2}$ . Following Kennicutt et al. (1989) we corrected the fluxes for foreground extinction only. For each galaxy, the  $E(B-V)$  used is listed in Table 1. Uncertainties in luminosity measurements result from uncertain distances, background removal, photometric calibration, internal extinction in the galaxy, selection of H II region boundaries, and clipping.

In the cases of several galaxies we have flux measurements of individual H II regions in common with measurements in the literature. We have compared several H II regions in these galaxies that are relatively bright and isolated. Except for DDO 167 our flux measurements are higher than those measured by Strobel et al. (1991) and Hodge et al. (1994b) for five galaxies. Our fluxes, adjusted for the same reddening correction, are on average 11% higher in DDO 50 to 53% higher for DDO 69. The exception is DDO 167, where our fluxes are on average 25% lower than those of Strobel et al. (1991). There are also two other galaxies for which the discrepancies are much larger. In IC10 we have compared our fluxes for Hodge & Lee's (1990) H II regions number 50 and 36 with our corresponding regions. When adjusted for the different reddening correction, our fluxes are 45 times higher. Furthermore, our region diameters, when adjusted for the same distance, are 6–10 times higher. The other galaxy that is quite discrepant is DDO 75, where we compare Hodge et al.'s (1994a) region number 17 with Aparicio & Rodríguez-Ulloa's (1992) region number 7 as well as our region. Our flux is 4 times higher than that of Aparicio & Rodríguez-Ulloa and 1.9 times higher than that of Hodge et al. We are very puzzled by these flux differences. Some variations are expected due to differences in choices of H II region boundaries and how deep the images go, but the particularly large differences are hard to explain and we do not know their cause. This is especially puzzling given the excellent consistency among our calibration constants between different objects and over many years. Like all astronomers we assume that our values are the correct ones, but in fact we do not have independent evidence to show that at this time. The one galaxy with additional independent measurements, DDO 50, is the one on which we all agree to within the uncertainties.

Understanding the detection limit for H II regions in each image is necessary in order to determine how far down the luminosity function is believable. For each galaxy image we added artificial H II regions using a stellar point spread function (PSF) determined from the unsubtracted H $\alpha$  image. The PSF radius that was used was about 2.5 times the FWHM of the stellar profile. We added a series of artificial H II regions stepped in integrated brightness, both in the outer parts of the galaxy and in the central region. We then clipped the image and looked to see what the faintest H II region was that would have been detected in our normal search process. By using a stellar profile, we are determining an upper limit to the detection limit since H II

regions with the same integrated brightness but spread out over a larger area or with a flatter distribution than that of a star could be missed. The detection limit, usually that of identifying an H II region within the central regions rather than in the outskirts, is listed in Table 2. The luminosity at which the H II region counts become incomplete could be somewhat higher than the detection limit.

### 3. THE H II REGION LUMINOSITY FUNCTION

#### 3.1. General Properties of the H II Region Luminosity Functions

The faintest H II region luminosities were measured to be around  $10^{35}$  ergs s $^{-1}$ , only a fraction of an Orion nebula ( $10^{37}$  ergs s $^{-1}$ , Kennicutt 1984). These low-luminosity regions represent regions ionized by single stars and density-bounded regions with significant photon loss. The most luminous region had a luminosity of  $8 \times 10^{39}$  ergs s $^{-1}$ , which is comparable to the luminosity of the 30 Doradus nebula in the Large Magellanic Cloud ( $7 \times 10^{39}$  ergs s $^{-1}$ , corrected only for foreground extinction and using a distance of 0.055 Mpc; Kennicutt 1984). The galaxies spanned a range of star formation rates; the galaxy with the fewest H II regions had only six, while the galaxy with the most had 204. The total number of H II regions that we have identified in each galaxy is listed in Table 2.

H II region luminosity functions were constructed for each of the galaxies, binned in logarithmic bins of 0.2 dex. The luminosity function is the logarithm of the number of regions counted in each bin divided by that bin size in ergs s $^{-1}$  and multiplied by  $10^{40}$  in order to make the numbers look nice. The luminosity functions for four galaxies, which represent typical luminosity functions for this sample, are shown in Figure 1. The luminosity functions for all of the galaxies in our sample are available in postscript graphic and ASCII tabular form in the electronic version of this journal. Over a large range of luminosities, luminosity func-

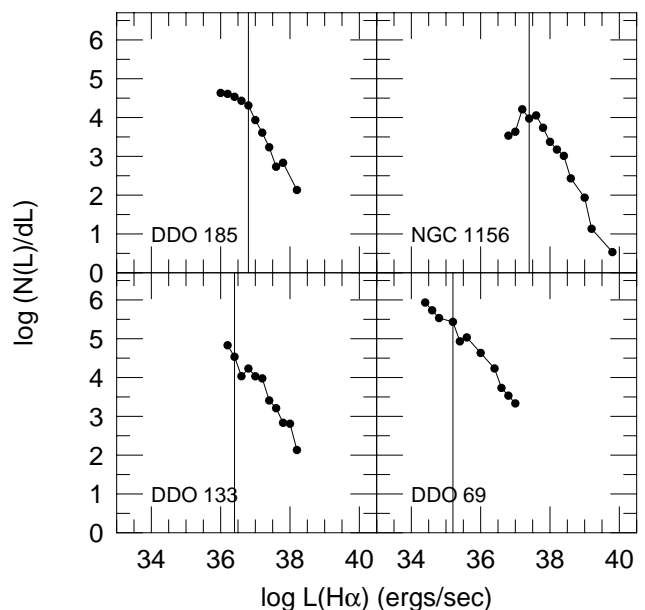


FIG. 1.—H II region luminosity functions for four normal Im galaxies. These galaxies represent the types of luminosity functions seen among the Im galaxies in our sample. The vertical line is the approximate detection limit for H II regions in the galaxy's central regions. H II regions detected below that limit are regions in less crowded areas of the galaxy and/or represent uncertainties in the measured fluxes.

tions can be fitted by the power law:  $N(L) = AL^a dL$ , where  $N(L)$  is the number of regions at luminosity  $L$  and  $dL$  is the bin size. This function has been successful in describing the luminosity functions for most galaxies in past studies. Although some of the fits to our galaxies were noisy as a result of small number statistics, most galaxies could be fitted reasonably well by this power function. The power-law indexes of these fits are listed in Table 2 along with the uncertainty in the fit. For most galaxies, the uncertainty in the index is  $\pm 0.1$ – $0.2$ . For three galaxies in common with Strobel et al. (1991), our power-law indexes are within  $\leq 1.5 \sigma$  of their values, although this still amounts to a 20%–40% difference.

### 3.2. Behavior of the H II Region Luminosity Functions

Many of the galaxies exhibit turnover, as do DDO 185 and NGC 1156 in Figure 1. In past studies, it has been suggested that this turnover point corresponds to the completeness limit. Incompleteness on the low end of the luminosity function is due to crowding and blending of fainter regions. Kennicutt et al. (1989) found that for most galaxies in their sample, this turnover point occurred between  $10^{36}$  and  $10^{37}$  ergs s $^{-1}$ . The turnover point for many of the galaxies in our sample is also in this luminosity range and is often consistent with the lower luminosity detection limits. The most likely interpretation, therefore, is that the turnover is due to incompleteness.

However, the luminosity functions for 12 of the 29 normal Im galaxies in this study do not exhibit turnover. These galaxies have been designated as “No Turnover” luminosity functions, while luminosity functions for which turnover was apparent are designated as “Turnover”, and these classifications are given in Table 2. For “Turnover” luminosity functions, the power-law index  $a$  was determined by excluding those bins fainter than the apparent turnover point.

“No Turnover” luminosity functions, such as those of DDO 69 and DDO 133 in Figure 1, often extend to very low luminosities, as shown in Figure 2, and as a group tend to have lower upper limits as well, as shown in Figure 3. Although there is a large overlap, the average upper luminosity cutoff for “Turnover” luminosity functions is  $1 \times 10^{38}$  ergs s $^{-1}$ , whereas the average upper luminosity cutoff for “No Turnover” luminosity functions is  $2 \times 10^{37}$  ergs s $^{-1}$ . “No Turnover” luminosity functions also tend to have small total numbers of H II regions. Most puzzling, however, is that the luminosity functions without turnovers are, on average, shallower than those with turnovers. The average power-law index for “Turnover” luminosity functions is  $a = -1.5 \pm 0.1$ , while the average power-law index for “No Turnover” luminosity functions is  $a = -1.0 \pm 0.1$ . The power-law index for “Turnover” luminosity functions is similar to the average value  $a = -1.7$  that Kennicutt et al. (1989) found for their sample of irregulars, to an average  $a = -1.5$  found by Strobel et al. (1991) for their sample, and within the uncertainties to the average  $a = -1.8 \pm 0.1$  found for a sample of four “dwarf” galaxies by Kingsburgh & McCall (1998) using a very different photometry method. Thus, the shallower power-law index of the “No Turnover” group of galaxies is more unusual.

The difference in the average slopes suggests the possibility of a physical rather than observational difference between the two types of luminosity functions. Since the “No Turnover” luminosity functions tend to cover low-

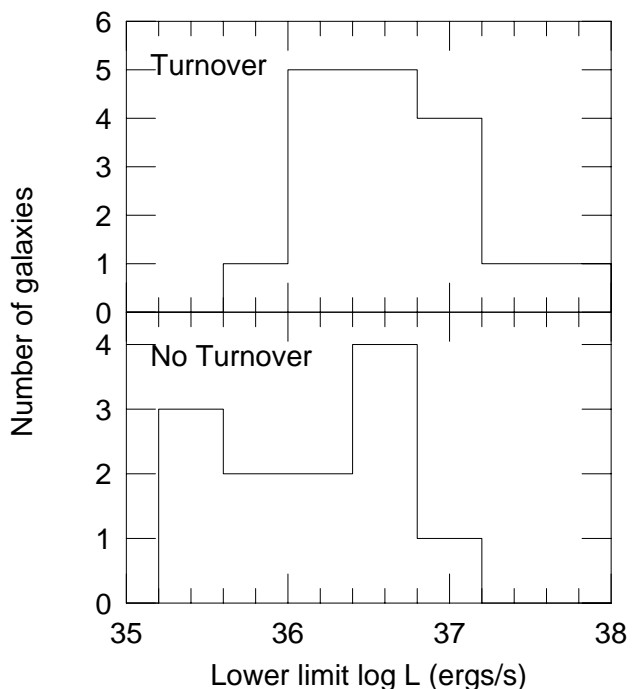


FIG. 2.—Lower limits to the H II region luminosity function for each galaxy as a function of the luminosity function type of that galaxy. “Turnover” galaxies exhibit some turnover; “No Turnover” galaxies do not. The lower limit luminosity is the faintest H II region detected or the lower detection limit, whichever is higher. For the functions with turnovers, the lower limit is the luminosity at the turnover point. Only the normal Im sample is shown.

luminosity regions and “Turnover” functions tend to be shifted to higher luminosities, the difference in slopes could represent differences in H II regions ionized by single or very small clusters of a few stars and those ionized by larger

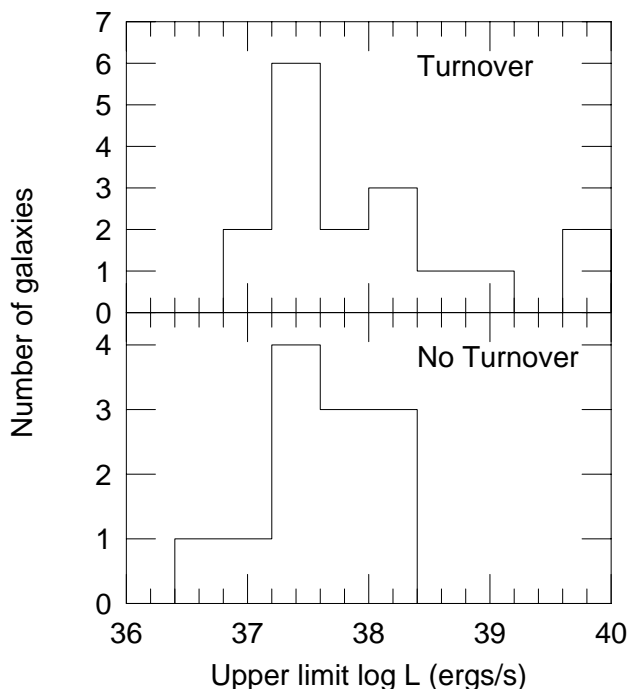


FIG. 3.—Upper limit to the H II region luminosity function for each galaxy as a function of the luminosity function type of that galaxy. “Turnover” galaxies exhibit some turnover; “No Turnover” galaxies do not. Only the normal Im sample is shown.

clusters of stars and OB associations. Walterbos & Braun (1992) also saw a flattening in the luminosity function of H II regions in M31 below  $10^{37}$  ergs s $^{-1}$ , and models by McKee & Williams (1997) and Oey & Clarke (1998) predict that a flattening should occur in the regime of regions ionized by single stars. The latter reference suggests that this occurs due to scatter resulting from a sparsely populated upper stellar mass function even when the parent population is the same. The break in the luminosity function is expected around the luminosity of the upper stellar mass limit of the stellar initial mass function  $\sim 10^{38}$  ergs s $^{-1}$  but can vary due to other factors as well. Thus, there are reasons to expect the luminosity function at lower H II region luminosities to be flatter than that at higher luminosities. Kennicutt et al. (1989) have also suggested that a break in the luminosity function that they saw in a subsample of their spiral galaxies around  $10^{39}$  ergs s $^{-1}$  corresponds to the transition between large clusters of stars and supergiant H II regions.

Interpreting the difference as physical, however, is complicated by the difficulty of obtaining accurate data at the low end of the luminosity function where incompleteness can be significant. However, galaxies with “No Turnover” luminosity functions also tend to have fewer regions overall and lower star formation rates per unit area (see Fig. 4), and detection limits are usually consistent with all but the faintest few points in the luminosity functions being believable. Therefore, incompleteness at low luminosities may not be as severe in these galaxies compared to busier systems. Another problem is due to the poorer statistics that result when there are fewer numbers of regions, as is the case in many “No Turnover” luminosity functions. However, here we make up for the smaller number of regions per galaxy with the large sample of galaxies. The dispersion in the slopes among the “No Turnover” group is no higher than that of the “Turnover” group, suggesting that the statistical uncertainties in the “No Turnover” luminosity functions are not significantly higher than those of the “Turnover” functions. Furthermore, the “No Turnover” class does include four galaxies with numbers of regions that are greater than the median value of 19 regions in the normal Im sample.

We, therefore, suggest that the difference in slope between the two luminosity function types is real. We identify two possible interpretations of this difference. The first is that the difference in luminosity functions represents a difference in the global ensemble of regions in “No Turnover” galaxies compared to “Turnover” galaxies. This could mean that galaxies with less star formation per unit area tend to have a flatter distribution of H II region luminosities but one that is skewed to lower luminosities overall. Alternatively, Oey & Clarke (1998) suggest that the aging of an ensemble of H II regions will also produce a difference in the slope in the sense that an older population of H II regions will have a flatter slope compared to a coeval, young population. This is what is seen in spiral galaxies: the interarm H II luminosity function is flatter and shifted to lower luminosities, peaking around  $10^{37}$ – $10^{37.5}$  ergs s $^{-1}$ , compared to that in the spiral arms themselves. Oey and Clarke contend that the interarm H II region population is an aging population, while that in the arms is younger. For the “No Turnover” galaxies this effect would mean that their star-forming activity is, on average, older than that in the “Turnover” galaxies.

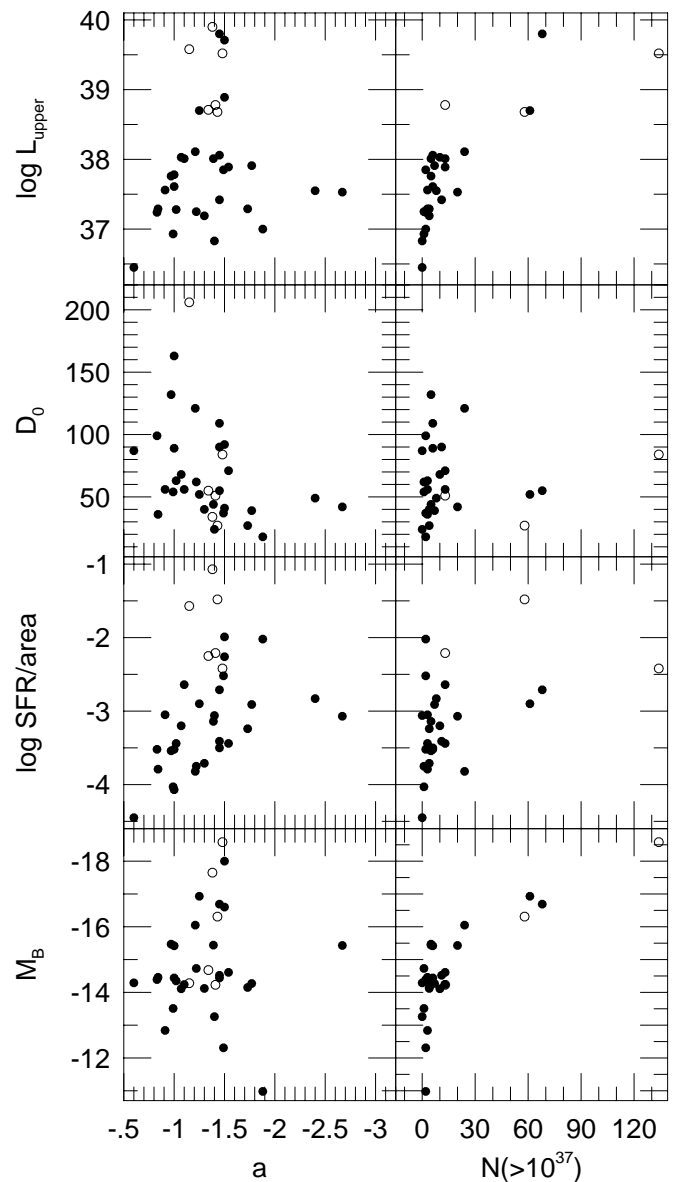


FIG. 4.—Power-law index  $a$  of the H II region luminosity function and number  $N(>10^{37})$  of regions with H $\alpha$  luminosities greater than or equal to  $10^{37}$  ergs s $^{-1}$  are plotted against properties of the galaxies. The SFR/area is the star formation rate per unit area given in Table 2,  $D_0$  is the characteristic diameter from the diameter distribution of each galaxy, and  $L_{\text{upper}}$  is the H $\alpha$  luminosity of the brightest H II region in each galaxy. Filled circles are normal Im galaxies included in this study, and open circles are our BCD and starburst sample.

The other possible interpretation of the difference in luminosity functions is that, because one type extends to lower luminosity H II regions, we are seeing two parts of the same universal luminosity function of irregulars and the part at lower luminosities has a different slope than that at higher H II luminosities. As noted above, this change in slope where regions are ionized by single or a few massive stars is predicted by models (McKee & Williams 1997; Oey & Clarke 1998). If true, this would then suggest that the turnovers seen in the “Turnover” luminosity functions may not in all cases be entirely due to incompleteness. We note that the luminosity functions of two “Turnover” galaxies with many regions (resulting presumably in better statistics) that extend to moderately low luminosities—DDO 47 and

NGC 2366—show a hint of beginning to turnover well before the estimated observational limit. This supports the difference between the two groups of luminosity functions as being that between the H II *regions*. On the other hand, not all luminosity functions of “No Turnover” galaxies extend to much lower luminosity H II regions (see, for example, Fig. 2). This supports the difference as being that between the *galaxies*.

However, the two groups of luminosity functions do overlap in luminosity. If we are sampling the same universal luminosity function and seeing differences between the bright end and the faint end, then we should see the two groups agree in certain restricted ranges of H II luminosity. To look at this we have determined the power-law indices in specific H II luminosity ranges for galaxies in each group. As we restrict the fit to fewer luminosity bins, the uncertainties in the fit to the power-law index go up. Thus, we have constrained the restricted fits to luminosity functions for which there are at least three points in the restricted luminosity range, the uncertainty in the resulting fit is less than 0.5, and the total number of regions in the galaxy is greater than the median value of 19 for the sample. These constraints are intended to ensure the statistical significance of our restricted power-law fits. However, another problem with the statistics is that there are fewer galaxies whose luminosity functions cover the specified range. There tend to be fewer “Turnover” galaxies when looking at the lower luminosity range and fewer “No Turnover” galaxies when looking at the upper luminosity range. We cannot do anything about this except to arrange our luminosity ranges such as to make sure that there are at least a few galaxies represented from both groups. Nevertheless, because of these problems the uncertainties in the individual power-law indices and averages is higher than for the unrestricted values.

First, we look at the bright end of the luminosity function and only include luminosity bins with luminosities  $\geq 10^{37}$  ergs s<sup>-1</sup>. The six “Turnover” galaxies give an average power-law index of  $a = -1.6 \pm 0.3$ , which is close to the unrestricted average of the entire group. There are two galaxies in the “No Turnover” category, and their average is  $a = -1.4 \pm 0.2$ . Thus, the average for the “No Turnover” luminosity functions has in fact steepened a bit from the unrestricted average of  $a = -1.1 \pm 0.1$  and is closer to the average for the “Turnover” group. If we restrict ourselves to luminosity bins  $\geq 10^{37.5}$  ergs s<sup>-1</sup>, the one “No Turnover” galaxy that satisfies our criteria has a power-law index of  $-1.6 \pm 0.4$ , which again is steeper than for the unrestricted fit. Because the power-law indices of the “No Turnover” galaxies become steeper and closer in value to that of the “Turnover” galaxies when restricted only to the brighter H II regions, this supports the idea that the two groups of luminosity functions are sampling different parts of the same universal luminosity function. However, the uncertainties, for the reasons noted above, are large, and the differences are at best a few sigma.

Second, we look at the low end of the luminosity function and only include luminosity bins with luminosities  $10^{36}$ – $10^{37}$  ergs s<sup>-1</sup>. The two “No Turnover” galaxies that satisfy our selection criteria have an average value of  $a = -1.1 \pm 0.2$ , which is the same as that of the unrestricted sample. The three “Turnover” galaxies, on the other hand, have an average value of  $a = -1.6 \pm 0.1$ , which is also similar to that of the unrestricted sample. If the two

types of luminosity functions were sampling the same function, we would have expected the “Turnover” luminosity functions to flatten out. This is not the case and by itself would support the idea that the two groups of galaxies are indeed different in terms of their large-scale star formation properties, whether sizes of regions or bulk ages.

Thus, these comparisons have yielded contradictory and, hence, inconclusive results perhaps because of poor statistics. We do not have the data to adequately distinguish between these two possibilities here. Below, however, we will *assume* that there is a universal luminosity function, at least for a given Hubble type of galaxy, when we construct a composite Im luminosity function for comparison with spirals. In that case we include all Im galaxies, both those with “Turnover” and those with “No Turnover” luminosity functions, to construct one universal Im galaxy luminosity function.

We have also explored whether there is any discernible difference in global properties between galaxies with steeper  $a$  or large numbers of H II regions and those with shallower  $a$  and smaller numbers of regions. We plotted the power-law index  $a$  and the number of H II regions with luminosities  $\geq 10^{37}$  ergs s<sup>-1</sup>  $N(>10^{37})$  against  $M_B$ , the star formation rate per unit area,  $D_0$  from the diameter distribution (described below), and the H $\alpha$  luminosity of the brightest H II region  $L_{\text{upper}}$  in each galaxy. These are shown in Figure 4. For  $a$ , there is a trend of steeper  $a$  for galaxies with higher normalized star formation rates. If a galaxy has more star formation per unit area, it tends to form more larger regions relative to smaller regions. There is also a trend between the characteristic diameter  $D_0$  with  $a$  such that the steeper the luminosity function the smaller  $D_0$ . This seems logical since the luminosity and diameter of H II regions should generally be related. We conclude from this and the discussion above that we do not understand what drives  $a$ , and we will attempt to address this in further studies. For  $N(>10^{37})$ , there is a trend of higher  $N$  for more luminous galaxies. This makes sense; the “bigger” the galaxy, the more H II regions. The trend, however, with star formation rate per unit area is very marginal at best.  $L_{\text{upper}}$  goes up as  $N(>10^{37})$  goes up: if a galaxy has more H II regions, it is more likely to make bigger ones too.

### 3.3. Galaxies with Lower Luminosity Truncations

There are three galaxies in our study that have lower limits to their H II region luminosity distributions that are significantly higher than their detection limits. The galaxies are DDO 155, whose faintest H II region is 20 times brighter than the expected limit; NGC 3738, whose faintest H II region is several times brighter; and NGC 1569, whose faintest region is 4 times brighter. These galaxies have high levels of star formation or the star formation is highly clumped, but our detection limits have been measured through the body of the galaxy and so should be representative of the galaxy. However, because of the clumpiness the limits are optimistic for the most concentrated regions of the galaxies. Nevertheless, there is also a limit to how many H II regions one can pack into a given volume of space. Therefore, we feel that these lower limits are most likely physical rather than entirely observational. There may be other galaxies with luminosity cutoffs at the faint end, but their cutoffs are masked by the detection limits.

While all galaxies are peculiar, DDO 155 and NGC 3738, classed here as normal Im galaxies, have their peculiarities



too. Both galaxies are tiny systems with relatively high star formation rates, and the star-forming regions are highly clumped. NGC 1569 has the highest star formation rate of any galaxy in our sample and is grouped with our BCD/starburst sample because it has a global star formation rate that is significantly elevated over the past rate (Gallagher, Hunter, & Tutukov 1984; Israel 1988). What is interesting is that the other five galaxies in the BCD/starburst sample do not exhibit this lower luminosity cutoff in spite of intense star formation. Haro 29 and Mrk 178 have H II regions down to  $10^{37}$  ergs  $s^{-1}$ , and NGC 4214, IC 10, and VIIZw 403 are cut off by the detection limit of less than  $10^{37}$  ergs  $s^{-1}$ . Thus, intense star formation does not mean that only the more luminous star-forming regions are formed.

### 3.4. Results from the H II Region Luminosity Functions

With our larger sample, our study confirms Kennicutt et al.'s (1989) conclusion that irregular galaxies do individually have generally shallower slopes than spiral galaxies. Kennicutt et al. (1989) measured a median power-law index of  $-1.9$  for Sbc-Sc spirals, while we measure  $-1.5 \pm 0.1$  and  $-1.0 \pm 0.1$  for our "Turnover" and "No Turnover" luminosity functions, respectively. This suggests that the number of H II regions at higher luminosities relative to that at lower luminosities is greater in irregular galaxies than in spiral galaxies. However, most of the irregular galaxies in this sample have upper cutoffs to their luminosity functions that are less than  $10^{38}$  ergs  $s^{-1}$ , far lower than that for spiral galaxies, indicating that an additional parameter is needed to characterize the difference between spirals and irregulars, as suggested by Kennicutt et al. (1989).

The luminosity of the most luminous H II region in each galaxy  $L_{\text{upper}}$  is given in Table 2. The range of  $L_{\text{upper}}$  is quite large. The most luminous H II region in NGC 2366 is 2000 times brighter than the most luminous region in DDO 216, and that in the starburst Im galaxy NGC 1569 is nearly 3000 times higher. Figure 5, a plot of  $L_{\text{upper}}$  and the number of H II regions per galaxy, suggests that the luminosity of the brightest H II region in the galaxy is tied to the total number of regions in the galaxy: those galaxies with the fewest regions also have the lowest  $L_{\text{upper}}$ . As we might expect, if there are only a few regions in the galaxy, the probability of having a supergiant H II region is smaller. Furthermore, the plot of the number of H II regions with luminosities greater than  $10^{37}$  ergs  $s^{-1}$  against the absolute magnitude of the galaxy in Figure 5 demonstrates that the number of regions in a galaxy is correlated with the absolute magnitude of the galaxy. There will be some scatter in this plot due to fluctuations in the star formation rate of a galaxy as it evolves since H $\alpha$  and  $M_B$  probe the star formation over different timescales; galaxies will move diagonally in the plot. The correlation between the number of regions and absolute magnitude of the galaxy continues as well for Kennicutt et al.'s Sc spirals.

Only two of the 29 normal Im galaxies included in this sample have 30 Doradus type supergiant H II regions. A supergiant H II region, defined here as  $L \geq 10^{39}$  ergs  $s^{-1}$ , will have the greatest impact on the surrounding interstellar medium as hundreds of massive stars concentrated in one place subject their surroundings to strong winds and supernova explosions. In contrast, five of the six irregulars included in Kennicutt et al.'s (1989) sample contain supergiant H II regions. This suggests that supergiant H II regions are rare for a more representative sample of noninteracting

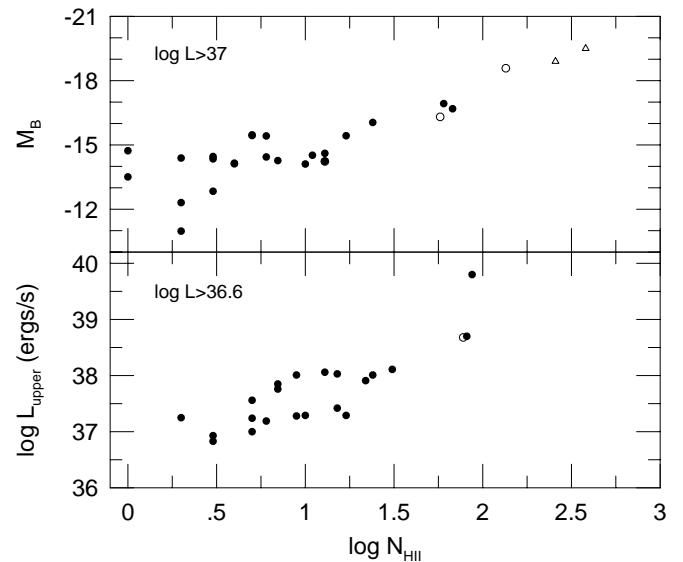


FIG. 5.—(Bottom) Relationship between the total number of H II regions in a galaxy and the luminosity of the most luminous H II region. Only the H II regions with luminosities greater than  $4 \times 10^{36}$  ergs  $s^{-1}$  were counted in order to avoid incompleteness but still be able to include most of the Im galaxies. (Top) Relationship between the total number of H II regions and the absolute blue magnitude of the galaxy. Here only H II regions with luminosities greater than  $10^{37}$  ergs  $s^{-1}$  were counted in order to allow spirals from Kennicutt et al. (1989) to be included. Filled circles are normal Im galaxies included in this study, and open circles are our BCD and starburst sample. Open triangles are Sc spirals from Kennicutt et al. that are complete to this H II luminosity limit.

irregular galaxies. The cause for the absence of supergiant H II regions in irregulars is most likely due to their small size (low absolute magnitude), which prevents these galaxies from forming lots of regions and that the presence of the rare supergiant H II region requires a larger statistical sample of H II regions to draw from. And, in fact, of the three normal Im galaxies with over 100 identified H II regions, two contain a supergiant H II region. Because there is one galaxy with many regions and no supergiant H II region, we can also conclude, therefore, that containing lots of H II regions is not a necessary condition for the presence of a supergiant H II region at a given instant of time.

However, this is not the case for the BCDs and starbursts. Of the six BCD and starburst irregulars three have made supergiant H II regions. Although one of our galaxies in this sample has both numerous H II regions and supergiant H II regions, there is also Haro 29, which contains only a few regions, one of which is a supergiant H II region, and IC 10, which contains many H II regions, none of which are quite luminous enough to be classed as a supergiant H II region. In the case of Haro 29, it is possible that the gas is concentrated toward the center of the galaxy as is the case in a small sample of other BCDs (van Zee, Skillman, & Salzer 1998), thus facilitating the formation of a supergiant H II region. The concentration of H I gas and formation of supergiant H II regions was also seen in a sample of amorphous galaxies (Hunter, van Woerden, & Gallagher 1994). As for the amorphous galaxies, the gas in Haro 29 could have piled up in the center as a result of a passing perturber that is now long gone, as in the models of Noguchi (1988a, 1988b).

Therefore, while supergiant H II regions may be part of the normal distribution of star-forming regions in irregu-

lars, most Im galaxies in fact do not contain supergiant H II regions. This means that most Im galaxies will not have that extreme level of disruption of the interstellar medium that is the consequence of such large star-forming regions. BCDs and starbursts, on the other hand, are more likely as a group to contain supergiant H II regions and suffer the consequences, but intense star formation does not guarantee the formation of such regions in these galaxies.

In Table 2 and Figure 6 we address the question of what size of regions contributes the bulk of the H II emission in these galaxies. In the table we include the fraction of emis-

sion from H II regions in each galaxy that is provided by supergiant H II regions ( $\geq 10^{39}$  ergs s $^{-1}$ ), *f*(30 Dor), and the fraction provided by nebulae comparable to Orion and fainter ( $10^{36}$ – $10^{37}$  ergs s $^{-1}$ ), *f*(Orion). Although supergiant H II regions make up a significant percentage of the flux for galaxies that have them (about 33% for NGC 1156 and 64% for NGC 2366), most irregular galaxies do not have regions this luminous. For eight of the 29 Im galaxies, over 50% of the H II luminosity comes from Orion-size and smaller H II regions, although this number could be somewhat higher as a result of incompleteness. The majority of the H II luminosity in the other galaxies comes from regions with luminosities  $10^{37}$ – $10^{38}$  ergs s $^{-1}$ .

Kennicutt et al. (1989) totaled the contribution of H II regions with luminosities greater than  $10^{38}$  ergs s $^{-1}$  and found that in their sample of irregulars 77% of the total H II region emission comes from these regions (their Table 3). For comparison, we have made the same calculation and show that number distribution in Figure 6 as well. We find that 19 of the Im galaxies have 0% contribution from regions  $\geq 10^{38}$  ergs s $^{-1}$ , with the rest ranging from 21% to 86%. The median value is 0%. Thus, among this more representative sample of Im galaxies, the irregulars do not continue the trend of early to late type spirals of an increasing fraction of emission coming from the largest regions. Among the BCD and starburst sample, however, this is not the case. There the percent contribution from regions  $\geq 10^{38}$  ergs s $^{-1}$  varies from 48% to 98% with a median value between 60% and 90%.

### 3.5. The Cumulative Luminosity Function

In their comprehensive study of H II region luminosity functions in spiral and irregular galaxies, Kennicutt et al. (1989) constructed a composite cumulative luminosity function each for Sb, Sc, and Im galaxies. That study showed Im galaxies to have the same luminosity distribution as the Sc galaxies, normalized to the galaxy luminosity, but with an increase in regions with H $\alpha$  luminosities greater than  $10^{39}$  ergs s $^{-1}$ . This suggestion that Im galaxies preferentially have more supergiant H II regions and the corresponding consequences that would have to the irregular galaxies prompted our investigation here with a larger sample of irregulars. We constructed a composite luminosity function for irregulars beginning at a lower H $\alpha$  luminosity limit of  $10^{36}$  ergs s $^{-1}$ . We used the detection limits given in Table 2 and locations of turnovers in individual luminosity functions to determine the faintest bin to which a given galaxy could contribute.

Initially, we constructed a composite cumulative luminosity function for our sample of irregulars and for our sample of BCD/starburst systems after the fashion of Kennicutt et al. (1989) so that we could compare directly with their published results. This involved summing in each luminosity bin all galaxies that were complete to a particular limiting luminosity, normalizing these groups of galaxies to the first galaxy group in the first two luminosity bins in common, summing the normalized groups of galaxies in each luminosity bin, and then normalizing each bin by the number of groups that contributed to it and by the sum of the luminosities of the galaxies that constituted the first group (to which everything was normalized). In Kennicutt et al.'s case there were only two such groups of galaxies: those that contributed  $\geq 10^{37}$  ergs s $^{-1}$  and those that contributed  $\geq 10^{38}$  ergs s $^{-1}$ . Here we have a range of limits

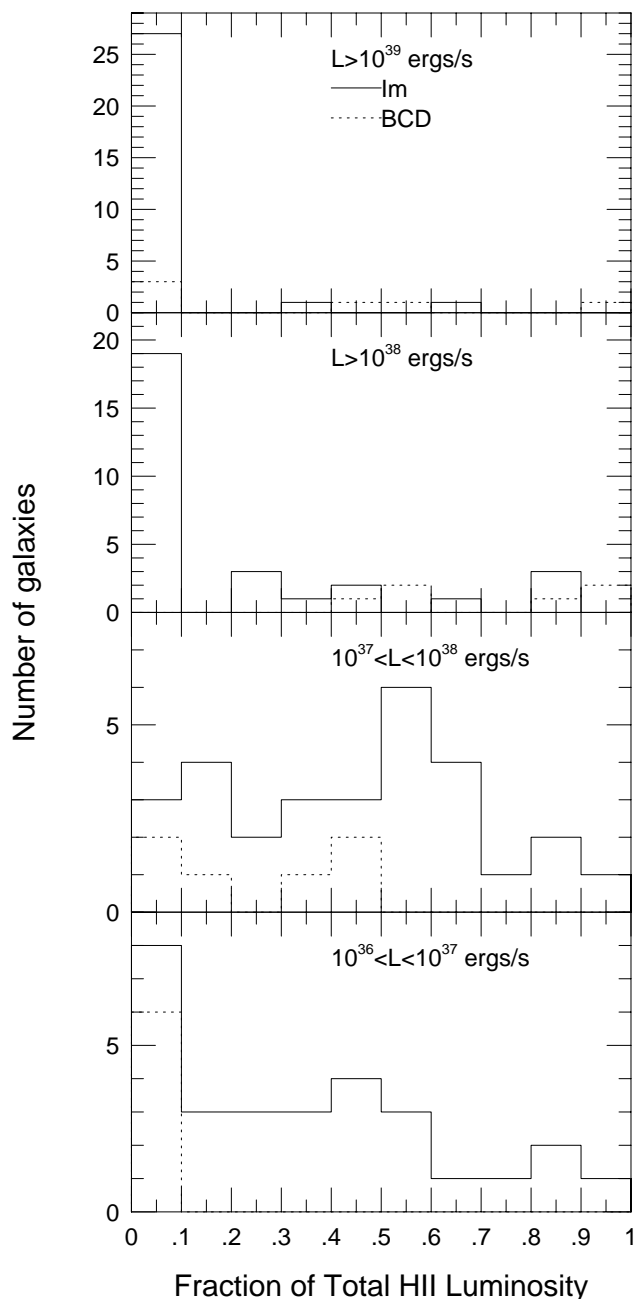


FIG. 6.—Fraction of total H II luminosity that is contributed by H II regions of a particular luminosity range: (a) supergiant H II regions with  $L \geq 10^{39}$  ergs s $^{-1}$ ; (b) giant H II regions with  $L \geq 10^{38}$  ergs s $^{-1}$  for comparison with Kennicutt et al. (1989); (c) regions ranging from luminosities like that of the Orion nebula up to 10 times brighter; and (d) regions comparable to Orion and down to 10 times fainter. The Im and BCD samples are shown separately.

from  $10^{36}$  ergs  $s^{-1}$  and up and many galaxies for which the upper limit falls below their cutoffs. To increase the statistics we want to include all systems. Therefore, we ended up with nine groups of galaxies. This method, modulo a constant, reproduced Kennicutt et al.'s results from the data that they give on the individual galaxies that they used.

However, we were dissatisfied with this method of combining the galaxies. This construction and normalization meant that some individual galaxies were weighted more or less than others depending on how many galaxies were in a particular galaxy group. Therefore, we then constructed a much simpler luminosity function in which each galaxy is added to all luminosity bins brighter than its faint limit and each luminosity bin is normalized by the sum of the luminosities of the galaxies that contributed to it, in units of  $10^{10} L_{\odot}$ . A galaxy was considered to contribute to all luminosity bins brighter than its faint limit. This means that we are adding in zeros for all bins where nothing is detected at higher luminosities and implies the assumption that the upper cutoff to the luminosity distribution in an individual small galaxy is statistical rather than physical. We also constructed composite luminosity functions in this fashion for Kennicutt et al.'s sample of Im, Sc, and Sb galaxies using their data. From this the cumulative luminosity function is constructed. The function for the BCD and starburst systems will be noisier since it has only six galaxies contributing to it, while the Im function has 29 galaxies.

The results are shown in Figure 7, where we plot our Im and BCD composite luminosity functions along with those that we constructed from Kennicutt et al.'s (1989) data for Sb, Sc, and Im galaxies. The functions constructed from

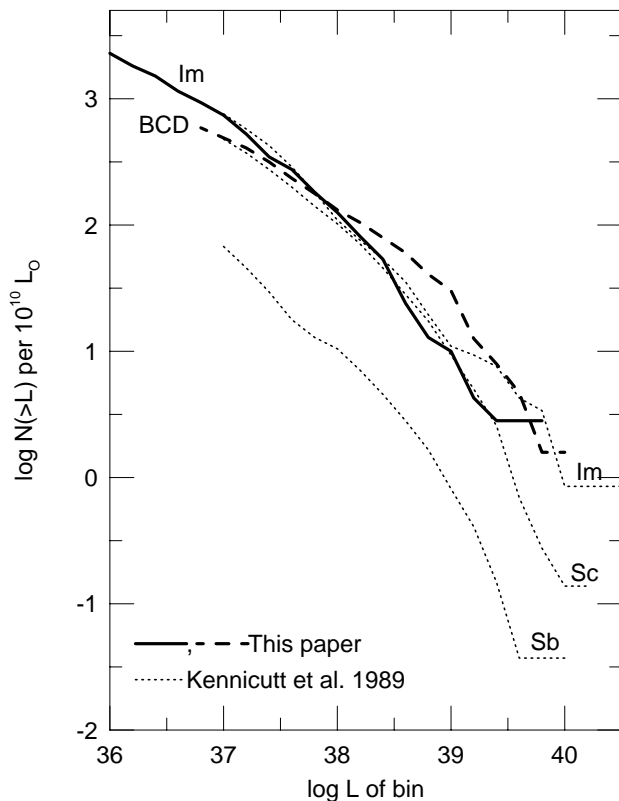


FIG. 7.—Composite cumulative luminosity functions for galaxies of different morphological type. The luminosity function is divided by the sum of the luminosities of the galaxies that contribute to it in units of  $10^{10} L_{\odot}$ .

Kennicutt et al.'s data can be compared to their Figure 8. What we find is that our Im sample is similar to within the uncertainties to Kennicutt et al.'s Sc and Im samples up to  $10^{39}$  ergs  $s^{-1}$ . Brighter than that our Im sample follows the Sc composite function rather than exhibiting the hump of extra supergiant H II regions that Kennicutt et al. saw in their Im sample (see also Kingsburgh & McCall's 1998). Thus, the intriguing suggestion that irregular galaxies preferentially contain more supergiant H II regions compared to Sc galaxies, relative to the luminosities of the galaxies, is not borne out when a larger, more representative sample of Im galaxies are examined. The BCD/starburst sample, on the other hand, does show an excess of H II regions with luminosities greater than  $10^{38}$  ergs  $s^{-1}$  compared to our Im sample and to Kennicutt et al.'s Sc sample. Thus, the BCD/starburst sample is making more of the intermediate and giant H II regions relative to their galaxy luminosity than an Sc or Im galaxy.

Although the Im galaxies do not contain an unusually large number of supergiant H II regions, a few galaxies do have unusually luminous single H II regions: the straight part of the Im line at high luminosity is the result of one region each in NGC 1156 and NGC 2366 and among the starbursts is one region in NGC 1569. The Kennicutt et al. (1989) sample of Im, Sc, and Sb galaxies exhibit this too at the top end of the luminosity function, but at higher H II luminosities. Im galaxies and even BCDs do not contain the most luminous H II regions that Sc galaxies contain. That is, the composite luminosity function of the Im and BCD galaxies is truncated at the high end compared to Sc galaxies.

#### 4. THE H II SIZE DISTRIBUTION

The cumulative H II region diameter distribution has been shown to follow the exponential function:  $N(>D) = N_0 e^{(-D/D_0)}$ , where  $N(>D)$  is the number of H II regions with a diameter larger than  $D$  and  $D_0$  is the characteristic diameter of the galaxy. The diameters were determined from the same regions outlined to measure the fluxes and were defined by  $D = 2(A/\pi)^{1/2}$ , where  $A$  is the area. Uncertainties in H II region diameters result from selection of H II region boundaries and distance measurements. The characteristic diameters were derived from the slopes of the diameter distributions using a least squares fit to  $\log N(>D)$  versus  $D$  and are listed in Table 2. The characteristic diameters ranged from 18 to 163 pc for the normal Im galaxies. For six galaxies in common with Strobel et al. (1991), the  $D_0$ , corrected to the same distance, are within  $\leq 2.5 \sigma$  except for two that are  $5 \sigma$  different. This corresponds to up to a 68% difference in the case of the most discrepant galaxy and a 14% difference in the case of the least discrepant.

Figure 8 demonstrates four typical diameter distributions and two of the common problems with these distributions. (The diameter functions for all of the galaxies in our sample are available in postscript graphic and ASCII tabular form in the electronic version of this journal.) The first problem, as shown by DDO 70 and DDO 133, is that there is a break in the diameter distribution. The bigger regions define a steeper slope than that of the smaller regions. The second problem, as shown by NGC 1156 and NGC 2366, is that the largest regions are too big for the distribution defined by the rest of the regions. This was also noted by Hodge (1983) and Miller & Hodge (1994) for their sample of galaxies. Other Im galaxies for which this was the case are DDO 53, DDO 75, DDO 87, DDO 126, DDO 168, and WLM. Among the

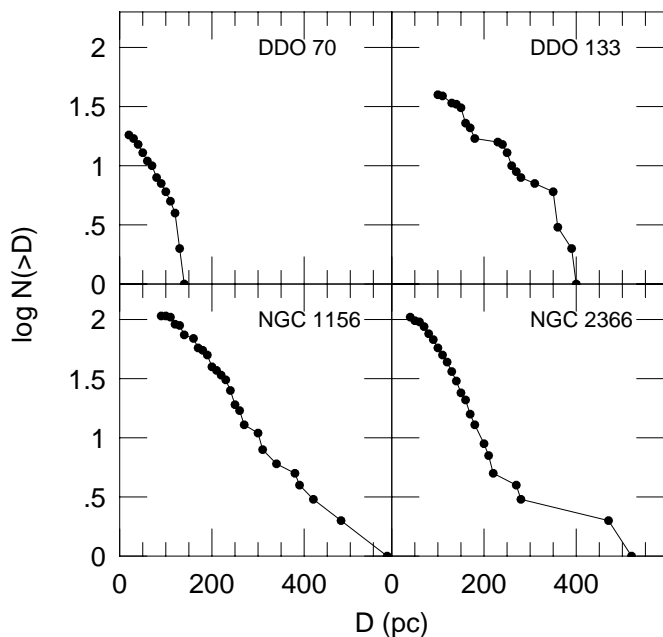


FIG. 8.—H II region diameter cumulative distributions for four representative Im galaxies.

BCD/starburst sample Haro 29, Mrk 178, NGC 1569, IC 10, and VII Zw 403 have this problem as well. These points were excluded when determining the slope of the diameter distribution. In fact, only DDO 43, DDO 47, DDO 69, DDO 115, DDO 125, DDO 154, DDO 155, DDO 165, DDO 216, and NGC 4214 have well-behaved diameter distributions within the uncertainties and when incompleteness at the small end is taken into account.

Because of these problems, our impression is that the exponential function is not particularly good at describing the distribution of sizes of star-forming regions in many irregular galaxies. We, therefore, tried several other functional fits:  $\log N$  versus  $\log D$ ,  $\log N$  versus  $D$ , and  $\log N(>D)$  versus  $\log D$ . However, in spite of its problems,  $\log N(>D)$  versus  $D$  was still the best fit compared to these.

Another complication to the diameter distribution is the possibility of a lower diameter cutoff. Most galaxies have H II regions down to the resolution of the H $\alpha$  images or lower size limits that are consistent with the luminosity detection limits. However, two galaxies have high lower size limits that could be physical: the H $\alpha$  image of DDO 155 has a resolution of 30 pc, but the smallest region that was identified has a diameter of 50 pc; the NGC 3738 image has a resolution of 54 pc, and the smallest region identified has a diameter of 140 pc. This is consistent with the truncation at the low-luminosity end of the luminosity distribution for H II regions in DDO 155 and NGC 3738 discussed above.

In terms of  $D_0$  there is no distinction between the Im sample and the BCD/starburst sample, at least when the discrepant largest H II region diameter bin is eliminated from the fit as described above. The average  $D_0$  for the Im sample is  $66 \pm 34$  pc, while that of the BCD/starburst sample is  $60 \pm 31$  pc. Even Haro 29's  $D_0$  of 110 pc is no larger than those of DDO 87, DDO 125, DDO 133, and DDO 169 in the Im galaxy sample.

Figure 9 demonstrates the weak correlation found previously by Strobel et al. (1991) between the absolute magnitude of the galaxy and its characteristic H II region

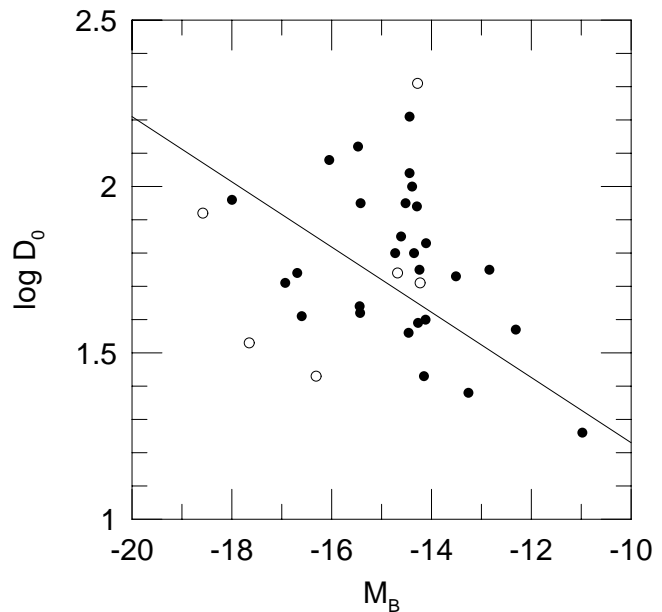


FIG. 9.—Relationship between the characteristic diameter of a galaxy and its absolute blue magnitude. Filled circles are Im galaxies, and open circles are the BCD/starburst sample. The line is the relationship determined by Strobel et al. (1991) for their sample of irregulars.

diameter. The brightest galaxies have the largest characteristic diameters and the faintest galaxies have the smallest characteristic diameters. Strobel et al. found that the galaxies in their sample were best fitted by the relation  $\log D_0 = 0.25(\pm 0.29) - 0.098(\pm 0.017)M_B$ . This line is plotted in Figure 9 along with our data. The galaxies in our sample are best fitted by the relation  $\log D_0 = 0.64(\pm 0.43) - 0.074(\pm 0.029)M_B$ , which is the same within the uncertainties as the fit by Strobel et al. However, the uncertainties are very high due to the large scatter in the plot. In fact, if we removed the faintest and brightest galaxies from the plot, the trend would mostly disappear. Thus, as Strobel et al. concluded, this is at best a very weak correlation.

We also investigated the correlation between  $N_0$  from the exponential fit and the integrated  $M_B$  of the galaxy.  $N_0$  represents the number of H II regions with a diameter greater than zero—in a sense, the total number of H II regions in the galaxy, so we might expect more luminous galaxies to have more regions as we found in Figure 5. This could also be the cause for the correlation between  $D_0$  and  $M_B$ . We would expect that galaxies with greater numbers of H II regions would produce more regions with large diameters, resulting in a larger characteristic diameter. However, no correlation was found between  $N_0$  and  $M_B$  (see also Hodge 1983) in spite of a correlation between  $N_{\text{H II}}$  and  $M_B$ .

In fact, we question the physical meaning of the  $N_0$  and  $D_0$  parameters. The characteristic diameter is problematic for several reasons. Often a linear fit to the higher end of the diameter distribution predicts a smaller characteristic diameter, while a linear fit to the lower end of the diameter distribution predicts a larger characteristic diameter. This is counterintuitive if  $D_0$  is really a “characteristic” size. Part of the reason for this problem is that the characteristic diameter assumes continuity in the diameter distribution, when, in reality, most diameter distributions exhibit at least an upper cutoff and most, as discussed above, exhibit different slopes for small and large regions. Thus, if the outer part

of the diameter distribution has a steeper slope than that for the smaller regions, it predicts large numbers of smaller regions that are not necessarily there, and hence  $D_0$  is small. As found in previous studies by Hodge (1983) and Miller & Hodge (1994), the slope of the diameter distribution does not accurately predict the size of the largest H II regions. Furthermore, it ignores the possibility of a true truncation at the smaller end of the diameter distribution, which we see evidence for in a few irregulars in our sample. For these reasons, we question the validity of the characteristic diameter and of  $N_0$  as physically meaningful parameters for many irregulars.

### 5. H II COMPLEXES

We have examined the question of what percentage of H II regions are found in H II complexes. We defined an H II region as being near another one if it is within  $1.35 \times (\text{radius of H II 1} + \text{radius of H II 2})$ . Then we defined a complex as the ensemble of all regions that were close to each other. The value 1.35 was arrived at by trial and error, determining by eye what looked reasonable on a few test galaxies. Some complexes consist of only two regions, while most contain many regions.

The results are plotted in Figures 10 and 11. For most galaxies  $\geq 80\%$  of the H II region luminosity is located in these complexes. However, the complexes themselves for the most part have modest luminosities. The typical H II complex has a luminosity of  $10^{37}$ – $10^{38}$  ergs s $^{-1}$ , comparable to up to 10 Orion nebulae.

That current sites of active star formation move around within an irregular galaxy over time and are often clumped on kiloparsec-size scales has been noted by Hodge (1969), Payne-Gaposchkin (1974), and Hunter et al. (1982). These H II complexes may be related to the star complexes discussed by Efremov (1995). Efremov has suggested that large-scale complexes of OB associations are a common mode of star formation in disk galaxies and that they are physical entities rather than chance collections. He argues that the star complex is the largest and initial scale of star formation that begins with gas superclouds of order  $10^7 M_\odot$ . A top-down scenario of star formation leads to individual giant molecular clouds within this region that form individual OB associations and clusters over an extended

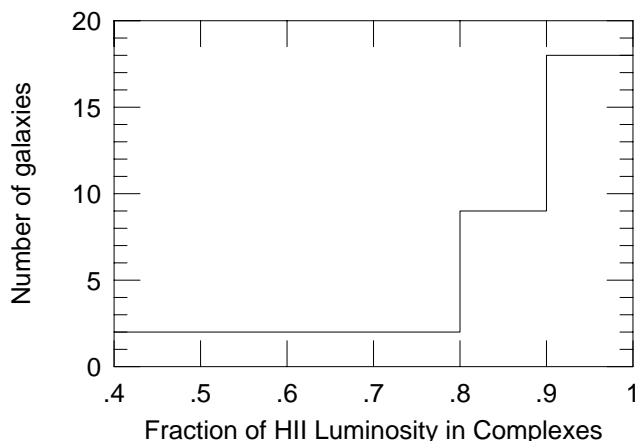


FIG. 10.—Number distribution of the fraction of the H II region luminosity that is found in H II complexes for each galaxy. This includes both Im and BCD/starburst samples.

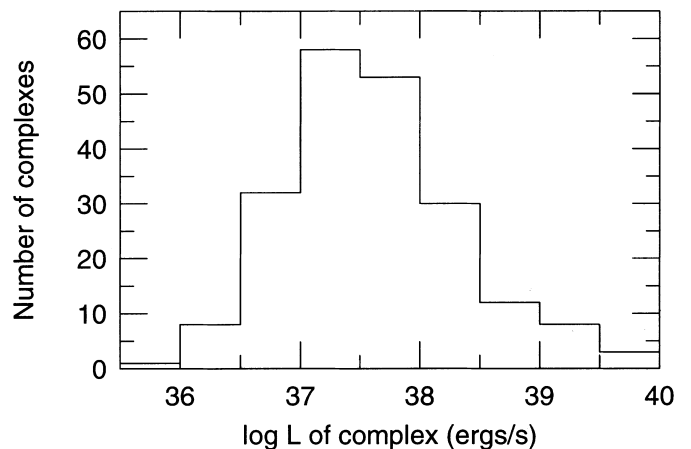


FIG. 11.—Number distribution of the H $\alpha$  luminosities of H II complexes. All complexes in all galaxies are combined including both Im and BCD samples.

period of time. These H II complexes may be the young versions of Efremov's star complexes.

### 6. SUMMARY

For a sample of 29 fairly normal, noninteracting Im galaxies, we find the following concerning the H II region luminosity and diameter distribution functions:

1. H II region luminosity functions for irregular galaxies are generally well fitted by a power law.
2. There are two types of luminosity functions: those that show turnover tend to have steeper power-law indexes and more H II regions, while those that do not show turnover tend to have fewer H II regions, shallower power-law indexes, and the H II regions are generally of low luminosity. If the luminosity function is universal for a given galaxy type, this difference suggests a possible break in the luminosity function at the transition between H II regions ionized by single stars and those ionized by clusters of stars. However, we cannot exclude the possibility that the two groups of galaxies are different in terms of their global star formation properties, either sizes of regions formed or bulk ages, perhaps coupled to the difference in star formation rates per unit area.
3. The luminosity functions for Im galaxies individually have shallower slopes than the luminosity functions for spiral galaxies, but frequently have much lower upper luminosity cutoffs.
4. Supergiant H II regions are rare in Im galaxies; this is probably because Im galaxies have fewer total numbers of H II regions, which is correlated with lower absolute magnitudes of the galaxies.
5. Most of the H II region luminosity comes from regions within a factor of 10 of the luminosity of the Orion nebula.
6. The composite cumulative luminosity function of all of the Im galaxies in this study is similar to that of Sc galaxies but truncated at the high-luminosity end. There is no excess of supergiant H II regions relative to the galaxy luminosity compared to Sc galaxies.
7. As seen previously, the correlation of characteristic diameter  $D_0$  and the absolute magnitude of the galaxy is very weak. However, many Im galaxy diameter distributions are not well fitted by an exponential function, and we question whether  $D_0$  and  $N_0$  are physically meaningful for many Im galaxies.

8. Over 80% of the H II region luminosity is in H II complexes, groups of  $\geq 2$  regions, and the luminosities of these complexes are generally  $\leq 10$  Orion nebulae.

9. Two Im galaxies show distributions that are truncated at the low-luminosity and low-diameter end. These are systems with high star formation rates and highly clumped H II regions.

For a sample of six BCD and starburst irregular galaxies, we find the following:

1. Supergiant H II regions are not as rare as they are in normal Im galaxies, even in systems with few overall regions, but neither are they always present in BCD/starburst galaxies.

2. Most of the H II luminosity comes from regions of order  $10 \times$  Orion nebula and larger.

3. The composite cumulative luminosity function of all of the BCD/starburst galaxies in this study is similar to that of Im and Sc galaxies to  $10^{38}$  ergs  $s^{-1}$ . Brighter than that the distribution shows an excess of H II regions relative to the galaxy luminosities. The distribution, however, is also truncated at the high end relative to Sc spirals.

4. Only one galaxy in this sample has an observed truncation in the luminosity function at the low end.

5. The characteristic diameters of the diameter distributions are similar to those found for the Im sample when fitted in the same way. However, like many of the Im galaxies, the largest H II regions are anomalously large for the rest of the distribution.

The question that motivated this study was whether irregular galaxies have an excess of supergiant H II regions relative to the galaxy luminosity compared to Sc galaxies as suggested by Kennicutt et al. (1989). We felt that our larger sample of noninteracting irregulars was more representative of the Im class than the systems that Kennicutt et al. had been constrained to use. We have, in fact, not confirmed their result and instead find that supergiant H II regions are rare in Im galaxies. Supergiant H II regions contain high concentrations of large numbers of roughly coeval massive stars and the combined winds and supernova explosions from those stars have a large impact on the surrounding interstellar medium. In particular the energy input from the

stars often blow large holes in the gas, thus rearranging the gas distribution—increasing the gas density in some places but also increasing the porosity of the interstellar medium. This could have profound implications for further star formation in that region of the galaxy, especially so in small galaxies like irregulars. The interstellar medium of irregulars that do make a supergiant H II region will undoubtedly be highly affected by the region (see, for example, the stunning H I map of the LMC produced by Kim et al. 1997). But, irregulars do not contain a disproportionate number of these regions for their size.

When one thinks of intense star formation such as that found in BCD or starburst galaxies, one also tends to think that the galaxy is dominated by supergiant H II regions. However, in our, admittedly small, sample of such systems, we did not find this to be the case. Surprisingly, although supergiant H II regions are more common in BCDs than in Im galaxies, supergiant H II regions rarely dominate the H II region distributions. However, the H II luminosity of BCDs is more dominated by larger regions than is the case for normal Im galaxies, and virtually all of the regions are located in complexes.

We are grateful to P. Hodge for comments on a draft of the paper. A. J. Y. would like to thank the National Science Foundation for providing funding for the Research Experiences for Undergraduates program, and Kathy Eastwood for directing the program at the Northern Arizona University. The H $\alpha$  imaging would not have been possible without filters purchased through funds provided by a Small Research Grant from the American Astronomical Society, National Science Foundation grant AST-9022046, and grant 960355 from JPL; for these funds we are most deeply grateful. D. A. H. wishes to thank Lowell Observatory for all the observing time that went into this project and for supporting the research. D. A. H. also acknowledges grant AST-9802193 from the National Science Foundation for funding the writing and publication of this work. This research has made use of the NASA/IPAC Extragalactic Database (NED), which is operated by the Jet Propulsion Laboratory, California Institute of Technology, under contract with the National Aeronautics and Space Administration.

## REFERENCES

- Aparicio, A., & Rodríguez-Ulloa, J. A. 1992, *A&A*, 260, 77  
 Burstein, D., & Heiles, C. 1984, *ApJS*, 54, 33  
 Cardelli, J. A., Clayton, G. C., & Mathis, J. S. 1989, *ApJ*, 345, 245  
 de Vaucouleurs, G., de Vaucouleurs, A., Corwin, H., Buta, R., Paturel, G., & Fouqué, P. 1991, *Third Reference Catalogue of Bright Galaxies* (New York: Springer)  
 Efremov, Y. N. 1995, *AJ*, 110, 2757  
 Gallagher, J. S., Hunter, D. A., & Tutukov, A. 1984, *ApJ*, 284, 544  
 Hodge, P. W. 1969, *ApJ*, 156, 847  
 ———, 1983, *AJ*, 88, 1323  
 Hodge, P. W., Kennicutt, R. C., & Strobel, N. V. 1994a, *PASP*, 106, 765  
 Hodge, P. W., & Lee, M. G. 1990, *PASP*, 102, 26  
 Hodge, P. W., Lee, M. G., & Kennicutt, R. C. 1989a, *PASP*, 101, 32  
 ———, 1989b, *PASP*, 101, 640  
 Hodge, P. W., Strobel, N. V., & Kennicutt, R. C. 1994b, *PASP*, 106, 309  
 Hunter, D. A., Gallagher, J. S., & Rautenkranz, D. 1982, *ApJS*, 49, 53  
 Hunter, D. A., Hawley, W. N., & Gallagher, J. S. 1993, *AJ*, 106, 1797  
 Hunter, D. A., & Hoffman, L. 1999, *AJ*, in press  
 Hunter, D. A., Light, R. M., Holtzman, J. A., Lynds, R., & O'Neil, E. J. 1997, *ApJ*, 478, 124  
 Hunter, D. A., van Woerden, H., & Gallagher, J. S. 1994, *ApJS*, 91, 79  
 Israel, F. P. 1988, *A&A*, 194, 24  
 Kennicutt, R. C. 1984, *ApJ*, 287, 116  
 Kennicutt, R. C., Balick, B., & Heckman, T. 1980, *PASP*, 92, 134  
 Kennicutt, R. C., Edgar, B. K., & Hodge, P. W. 1989, *ApJ*, 337, 761  
 Kim, S., Freeman, K. C., Staveley-Smith, L., Sault, R. J., Kesteven, M. J., & McConnell, D. 1997, *Proc. Astron. Soc. Australia*, 14, 119  
 Kingsburgh, R. L., & McCall, M. L. 1998, *AJ*, 116, 2246  
 Larson, R. B. 1983, *Highlights Astron.*, 6, 191  
 Lynds, R., Tolstoy, E., O'Neil, E. J., & Hunter, D. A. 1998, *AJ*, 116, 146  
 Massey, P. 1998, in *ASP Conf. Ser.* 142, *The Stellar Initial Mass Function* (38th Herstmonceux Conference), ed. G. Gilmore & D. Howell (San Francisco: ASP), 17  
 Massey, P., & Hunter, D. A. 1998, *ApJ*, 493, 180  
 Massey, P., Johnson, K. E., & DeGioia-Eastwood, K. 1995a, *ApJ*, 454, 151  
 Massey, P., Lang, C. C., DeGioia-Eastwood, K., & Garmany, C. D. 1995b, *ApJ*, 438, 188  
 McKee, C. F., & Williams, J. P. 1997, *ApJ*, 476, 144  
 Miller, B. W., & Hodge, P. W. 1994, *ApJ*, 427, 656  
 Noguchi, M. 1988a, *A&A*, 201, 37  
 ———, 1988b, *A&A*, 203, 259  
 Oey, M. S., & Clarke, C. J. 1998, *AJ*, 115, 1543  
 Oey, M. S., & Massey, P. 1995, *ApJ*, 452, 2100  
 Payne-Gaposchkin, C. 1974, *Smithsonian Contrib. Astrophys.* 16  
 Strobel, N. V., Hodge, P. W., & Kennicutt, R. C. 1991, *ApJ*, 383, 148  
 van Den Bergh, S. 1981, *AJ*, 86, 1464  
 van Zee, L., Skillman, E. D., & Salzer, J. J. 1998, *AJ*, 116, 1186  
 Walterbos, R. A., & Braun, R. 1992, *A&AS*, 92, 625